Journal of Electromagnetic Waves and Applications

ISSN: 0920-5071 (Print) 1569-3937 (Online) Journal homepage: www.tandfonline.com/journals/tewa20

Electromagnetic interference from shielding effectiveness of a rectangular enclosure with apertures – circuital approach, FDTD and FIT modelling

H. Azizi, F. Tahar Belkacem, D. Moussaoui, H. Moulai, A. Bendaoud & M. Bensetti

To cite this article: H. Azizi, F. Tahar Belkacem, D. Moussaoui, H. Moulai, A. Bendaoud & M. Bensetti (2014) Electromagnetic interference from shielding effectiveness of a rectangular enclosure with apertures – circuital approach, FDTD and FIT modelling, Journal of Electromagnetic Waves and Applications, 28:4, 494-514, DOI: 10.1080/09205071.2013.875862

To link to this article: https://doi.org/10.1080/09205071.2013.875862

Journal of Electromagnetic Waves and Applications, 2014
Vol. 28, No. 4, 494–514, http://dx.doi.org/10.1080/09205071.2013.875862

Taylor & Francis
Taylor & Francis Group

Electromagnetic interference from shielding effectiveness of a rectangular enclosure with apertures – circuital approach, FDTD and FIT modelling

H. Azizi[a], F. Tahar Belkacem[b], D. Moussaoui[b], H. Moulai[a]*, A. Bendaoud[c] and M. Bensetti[d]

[a]*Electrical Engineering, University of Science and Technology Houari Boumediene, FEI/LSEI, BP 32 El Alia, Algiers 16311, Algeria;* [b]*Electromagnetic Systems Laboratory, EMP Bordj El-bahri, Algiers 16111, Algeria;* [c]*ICEPS Laboratory, University of Sidi Belabbes Djillali Lyabes, BP 89 22000, Sidi Belabbes, Algeria;* [d]*ESIGELEC-Irseem Laboratory, BP 10024, Saint Etienne du Rouvray, Saint Etienne 76801, France*

(*Received 8 July 2013; accepted 11 December 2013*)

Apertures in a rectangular enclosure can be the coupling path of electromagnetic interference. This paper is devoted to the development of approximating phenomenological models in order to estimate the electromagnetic energy coupling through apertures into enclosures. The effect of apertures on shielding effectiveness (SE) of the enclosure is studied with both circuit modelling method and the finite-difference time-domain (FDTD) method. The results of SE predictions obtained by the analytical formulation and FDTD method are compared and validated with full-field simulations using the software CST/EMC. The software code is based on the finite integration technique. The investigation includes accurate calculation of both magnetic and electric shielding as a function of frequency, enclosure dimensions, apertures shapes, position within the enclosure, plane wave incidence mode and the "loaded aperture" approach.

Keywords: electromagnetic compatibility; shielding effectiveness; enclosures; circuital approach; FDTD; FIT

Introduction

Recently, as the electronic industry makes remarkable progress with the high technologies in the field of electronics, the structure of high-speed electronic equipments and components including chips, PCBs and packages becomes more and more complex. Also, as modern high-speed digital systems marks gigahertz ear in clock cycle, the system bus speed of computer systems becomes increasingly fast. Accordingly, the system requirements related to the signal integrity or electromagnetic interference such as the timing budgets, the noise margin and the radiated emission/immunity must be much tighter.

Electromagnetic shielding is frequently used to reduce the emissions or improve the immunity of electronic equipments. The performance of a shielding enclosure is quantified by its shielding effectiveness (SE) defined as the ratio of field strengths in the presence and absence of the enclosure. Due to the great number of applications of

*Corresponding author. Email: hmoulai@usthb.dz

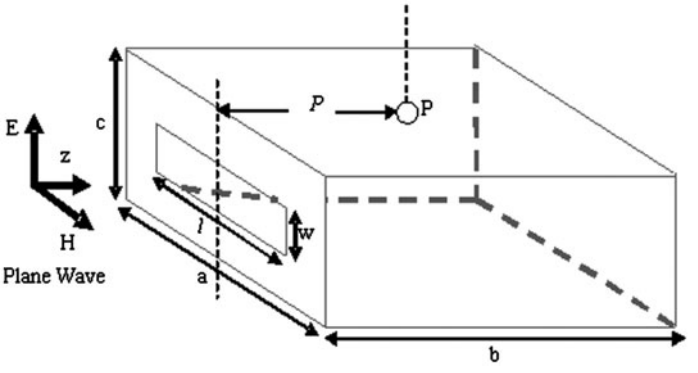

Figure 1. Geometry of the test enclosure.

shielding devices in the electronic industry, there is a great interest in the development of evaluation methods of the SE. In a real device, an enclosure has many apertures for input and output connections, control panels, ventilation panels and so on. However, at the same time, these apertures are responsible for a dramatic degradation of the SE. Therefore, it is mandatory, from an EMC point of view, to take into account the apertures effects (Figure 1).

The ability of a shielding enclosure is characterized by its SE which is a function of frequency. The SE of cavities with apertures has been studied with different methods: analytical formulations or numerical technique. Analytical ways provide much faster means of calculation of SE and enable the effect of design parameters to be investigated. One of the first successful techniques was proposed by Robinson et al. [1], who used an equivalent circuit technique to find sufficiently accurate results. This straight forward approach is limited to centred apertures such as the incident plane wave can only have one polarization direction and ignores the mutual admittance between the apertures.

Numerical methods have been widely applied to solve different types of electromagnetic scattering problems, but they often require much computing time and memory. The methods that are used for predicting the shielding of a particular enclosure and easy for designers in their investigations include transmission-line matrix,[2] finite-difference time-domain (FDTD),[3–5] finite integration technique (FIT),[6,7] finite-element time-domain method,[8] moments method[9] and a hybrid moment method/FDTD approach which was reported in [9,10] and applied to coupling and penetration into complex structures.

Circuit modelling method

Metallic shields are widely used to solve both susceptibility and emission problems of electrical and electronic systems. Due to the great number of applications of shielding devices in the electronic industry, there is a great interest in the development of methods that is able to evaluate the penetration of an electromagnetic field inside a metallic enclosure with apertures.

An analytical model will be first presented. It is useful to evaluate the SE of a rectangular metallic enclosure with a rectangular aperture. The aperture is modelled as

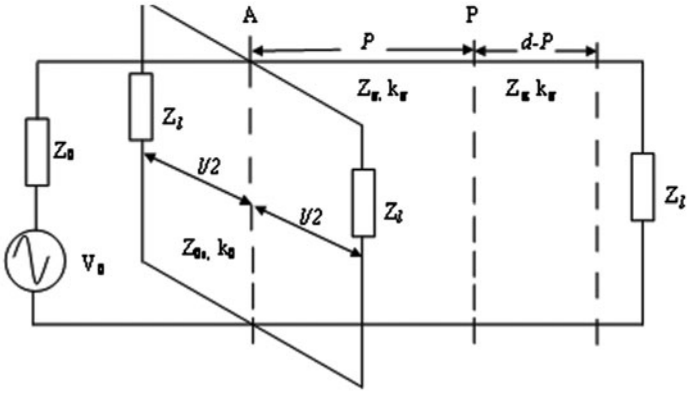

Figure 2. Equivalent circuit.

a coplanar transmission line and the enclosure is modelled as a length of a rectangular waveguide ended by a short circuit. The effects of the incident electromagnetic wave are taken into account by using suitable forcing terms in the equations related to the aperture model.

A rectangular aperture in an empty rectangular enclosure is represented by the equivalent circuit presented by Robinson et al. [1], which is shown in Figure 2. The longer side of the slot is shown normal to the E-field, which is the worst case for shielding.

The electric shielding at a distance p from the slot is obtained from the voltage at point P in the equivalent circuit, while the current at P gives the magnetic shielding. The radiating source is represented by the voltage V_0 and impedance $Z_0 = 377\ \Omega$ and the enclosure by the shorted waveguide whose characteristic impedance and propagation constant are Z_g and K_g. The load impedance Z_l is included in this circuit model, which represents the loss of enclosure.

Slot impedance

The aperture is represented as a length of a coplanar strip transmission line, shortened at each end (This consideration is founded on the basis that the electromagnetic field along the aperture makes propagating and circulating the induced currents generated around this aperture). The total width is equal to the height of the enclosure b and the separation is equal to the width of the slot w. Its characteristic impedance is given by Gupta et al. [11] as:

$$Z_{0s} = 120\pi K(w_e/b)/K'(w_e/b) \tag{1}$$

where K and K' are elliptic integrals. The effective width w_e is given by:

$$w_e = w - \frac{5t}{4\pi}\left(1 + \ln\frac{4\pi w}{t}\right) \tag{2}$$

where t is the thickness of the enclosure wall. If $w_e < b/\sqrt{2}$ (which is true for most practical apertures) then, according to Gupta et al., the following approximation can be used:

$$Z_{0s} = 120\pi^2 \left[\ln \left(2 \frac{1 + \sqrt[4]{1 - (w_e/b)^2}}{1 - \sqrt[4]{1 - (w_e/b)^2}} \right) \right]^{-1} \tag{3}$$

To calculate the aperture impedance Z_{ap}, we transform the short circuits at the ends of the aperture through a distance $l/2$ to the centre. This is represented by point A in the equivalent circuit. It is necessary here to include a factor l/a in order to take into account the coupling between the aperture and the enclosure:

$$Z_{ap} = \frac{1}{2} \frac{l}{a} j Z_{0s} \tan \frac{K_0 l}{2} \tag{4}$$

This formulation represents the relationship between transmission line and waveguide theory.

Electric and magnetic SE

From Thevenin's theorem and combining between Z_0, V_0 and Z_{ap}, one obtains an equivalent voltage:

$$V_1 = V_0 Z_{ap} / \left(Z_0 + Z_{ap} \right) \tag{5}$$

And the source impedance:

$$Z_1 = Z_0 Z_{ap} / \left(Z_0 + Z_{ap} \right) \tag{6}$$

For the TE_{10} propagation mode, the waveguide will have the following characteristic impedance:

$$Z_g = Z_0 \Big/ \sqrt{1 - (\lambda/2a)^2} \tag{7}$$

And propagation constant:

$$k_g = k_0 \sqrt{1 - (\lambda/2a)^2} \tag{8}$$

where

$$k_0 = 2\pi/\lambda \tag{9}$$

Note that Z_g and k_g are imaginary at frequencies below the cut-off (equal to $c_0/2a$).

Now, we transform V_1, Z_1 and the short circuit at the end of the waveguide to P, giving an equivalent voltage V_2, source impedance Z_2 and load impedance Z_3 as follows:

$$V_2 = \frac{V_1}{\cos k_g p + j \left(Z_1 / Z_g \right) \sin k_g p} \tag{10}$$

$$Z_2 = \frac{Z_1 + j Z_g \tan k_g p}{1 + j \left(Z_1 / Z_g \right) \tan k_g p} \tag{11}$$

$$Z_3 = j Z_g \tan k_g (d - p) \tag{12}$$

The voltage at P is now:

$$V_p = V_2 Z_3/(Z_2 + Z_3) \tag{13}$$

And the current at P is:

$$i_p = V_2/(Z_2 + Z_3) \tag{14}$$

In the absence of the enclosure, the load impedance at P is simply Z_0. The voltage at P is:

$$V'_p = V_0/2 \tag{15}$$

And the current is:

$$i'_p = V_0/2Z_0 \tag{16}$$

The electric and magnetic shielding (SM) are therefore given by:

$$SE = -20\log_{10}|V_p/V'_p| = -20\log_{10}|2V_p/V_0| \tag{17}$$

$$SM = -20\log_{10}|i_p/i'_p| = -20\log_{10}|2i_pZ_0/V_0| \tag{18}$$

FDTD method

The FDTD method has been extensively used way to predict the electromagnetic behaviour of various guided waves and radiation structures.[3–5,12–14] It possesses the advantages of simple implementation for relatively complex problems, high accuracy and the ability of work with a wide range of frequencies, stimuli, objects, environments and response locations. A disadvantage of the FDTD method is that, because of the time-domain formulation, computations on resonant structures lead to prohibitively long computation times, and that significant computational resources are expended for modelling an electrically small object without the aid of special sub-cellular or multi-grid algorithms.

FDTD objects are defined by specifying dielectric and magnetic material parameters at the calculated electric and magnetic field locations. This method is based on the discretization of two Maxwell's equations directly in time and spatial domains and

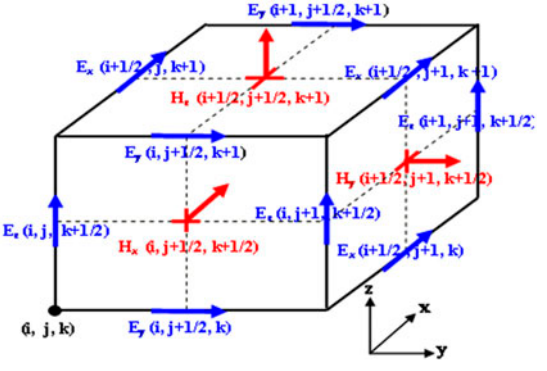

Figure 3. Positions of the field components in unit Yee cell.

dividing the volume of interest into unit (Yee) cells (Figure 3).[3] These equations can be written in loss regions with sources as:

$$\frac{\partial \vec{E}}{\partial t} = \frac{1}{\varepsilon}\nabla \times \vec{H} - \frac{\sigma}{\varepsilon}\vec{E} \tag{19}$$

$$\frac{\partial \vec{H}}{\partial t} = \frac{1}{\mu}\nabla \times \vec{E} - \frac{\rho'}{\mu}\vec{H} \tag{20}$$

where

$$\vec{B} = \mu\vec{H} \tag{21}$$

$$\vec{D} = \varepsilon\vec{E} \tag{22}$$

$$\vec{J}_e = \sigma\vec{E} \tag{23}$$

$$\vec{J}_m = \rho'\vec{H} \tag{24}$$

$\vec{B}$, $\vec{D}$, $\vec{E}$, $\vec{H}$, $\vec{J}_m$ and $\vec{J}_e$ are the electric flux density, magnetic flux density, electric field, magnetic field, impressed magnetic current density and impressed electric current density vectors, respectively.

FDTD technique uses simple central-difference approximations to evaluate the space and time derivatives. It is a time stepping procedure. Inputs are time-sampled analog signals. The region being modelled is represented by two interleaved grids of discrete points.

By staggering the discrete electric and magnetic fields in space and time, this leads to a second-order accurate approximation, from which an explicit update scheme can be derived. For example, the explicit update expressions for E_x and H_x are:

$$\begin{aligned} E_x^{n+1}(i+1/2,\ j,k) = {} & Ca(i+1/2,j,k)\cdot E_x^n(i+1/2,\ j,k) + \frac{Cb(i+1/2,\ j,k)}{\Delta y} \\ & \cdot [H_z^{n+1/2}\,(i+1/2,\ j+1/2,k) - H_z^{n+1/2}\ (i+1/2,\ j-1/2,k)] \\ & + \frac{Cb(i+1/2,\ j,k)}{\Delta z}\cdot [H_y^{n+1/2}\,(i+1/2,\ j,k-1/2) \\ & - H_y^{n+1/2}\,(i+1/2,\ j,k,+1/2)] \end{aligned} \tag{25}$$

$$\begin{aligned} H_x^{n+1/2}(i,\ j+1/2,k+1/2) = {} & Da(i,\ j+1/2,k+1/2)\cdot H_x^{n-1/2}(i,\ j+1/2,k+1/2) \\ & + \frac{Db(i,\ j+1/2,k+1/2)}{\Delta z}\cdot \Big[\Big(E_y^n\,(i,\ j+1/2,k+1) \\ & - E_y^n\,(i,\ j+1/2,\ k)\Big)\Big] + \frac{Db(i,\ j+1/2,k+1/2)}{\Delta y} \\ & \cdot [E_z^n\,(i,\ j,\ k+1/2) - E_z^n\,(i,\ j+1,k,+1/2)] \end{aligned} \tag{26}$$

where

$$Ca_{(i,j,k)} = \left(1 - \frac{\sigma_{(i,j,k)}\cdot\Delta t}{2\varepsilon_{(i,j,k)}}\right) \Big/ \left(1 + \frac{\sigma_{(i,j,k)}\cdot\Delta t}{2\varepsilon_{(i,j,k)}}\right) \tag{27}$$

$$Cb_{(i,j,k)} = \left(\frac{\Delta t}{\varepsilon_{(i,j,k)}}\right) / \left(1 + \frac{\sigma_{(i,j,k)} \cdot \Delta t}{2\varepsilon_{(i,j,k)}}\right) \tag{28}$$

$$Da(i,j,k) = \left(1 - \frac{\rho'(i,j,k) \cdot \Delta t}{2 \cdot \mu(i,j,k)}\right) / \left(1 + \frac{\rho'(i,j,k) \cdot \Delta t}{2 \cdot \mu(i,j,k)}\right) \tag{29}$$

$$Db(i,j,k) = \left(\frac{\Delta t}{\mu(i,j,k)}\right) / \left(1 + \frac{\rho'(i,j,k) \cdot \Delta t}{2 \cdot \mu(i,j,k)}\right) \tag{30}$$

A rectangular three-dimensional grid of $53 \times 75 \times 48$ cells is used as the computational domain. A higher resolution was chosen more accurately to model apertures associated with this configuration.

By choosing a value of spatial increment lower or equal to $\lambda/10$ (Δx, Δy and $\Delta z \leq \lambda/10$), it becomes correct to say that the phenomenon of dispersion is negligible. By reason of this criteria of dispersion, the sampling must be sufficiently fine and regular ($\Delta x = \Delta y = \Delta z$) to be able to follow the temporal evolution of the electromagnetic field.

The spatial increments in the x, y and z directions are $\Delta x = \Delta y = \Delta z = 10.8$ mm, the time step associated with this spatial increment dimension is:

$$\Delta t = \frac{\Delta x}{2 \times c} = \frac{0.018}{2 \times (3 \times 10^8)} = 3 \times 10^{-11} s \tag{31}$$

The simulations require typically from 12,000 to 15,000 time steps to achieve the steady state. The simulation was carried out on a 4 GB memory, 3.66 GHz processor speed computer for 9 h. The Hamming windowing was used to smooth the obtained data before applying the Fourier transform to these data in order to obtain the frequency-domain characteristics.

CST software

The developed FDTD technique and obtained results are validated by comparing the SE predictions with full-field simulations using the CST software.

CST software, which is available from IRSEEM laboratory, is a specialized tool for the 3D EM simulation of high frequency components. The software code is based on the FIT.[6]

The FIT is a consistent discretization scheme for Maxwell's equations in their integral form. The resulting matrix equations of the discretized fields can be used for efficient numerical simulations on modern computers. In addition, the basic algebraic properties of this discrete electromagnetic field theory allow to prove analytically and algebraically the conservation properties with respect to the energy and charge of the discrete formulation, and gives an explanation of the stability properties of numerical formulations in the time domain.

The computational time by CST software is of about 40 min, on a 3.66 GHz PC with 4GB of RAM. However, the computational time by the analytical method is of about 1 min with the same means of calculation.

Geometry of the tested enclosure

The rectangular enclosure tested is shown in Figure 1. It consists of an aluminium box with $50 \times 40 \times 70$ cm dimensions and a 25×10 cm aperture. Five walls of the box are

carefully welded together to ensure that there is no leakage through these parts of the box. The electric and magnetic shielding at a distance p from the slot is obtained from the electric and magnetic field at point P.

Definition of SE

SE is used to value the effect of shielding in electromagnetic coupling problems of cavities with apertures. The definition of SE is based on a plane wave excitation and the following procedure [12]:

- Excite the cavity with an incident pulse plane wave and record the electric field at the position of interest.
- Excite an empty space computational domain with the same incident pulse plane wave and record the electric field at the position of interest.
- Fourier transform of the time-domain data.
- Compute the SE in decibels.

SE is defined as the ratio of the electric fields and SM of magnetic fields such as:

$$SE = 20 \log \frac{Ez_0}{Ez_1} \tag{32}$$

$$SM = 20 \log \frac{Hx_0}{Hx_1} \tag{33}$$

where Ez_0, the electric field strength with the shield; Ez_1, the electric field strength in the absence of the shield; Hx_0, the magnetic field strength with the shield; Hx_1, the magnetic field strength in the absence of the shield.

The commercial CST software or the difference finite method when directly applied to Maxwell's equations enables accurate modelling thanks to an exact formulation of the electromagnetic waves propagation phenomena in the computational domain. On the other hand, the analytical model is based on transmission lines method which assumes the metallic enclosure as an equivalent electrical circuit that allows the Thevenin's theorem application in order to calculate the voltage V and current I that represent the electric and magnetic fields, respectively, at point P inside the enclosure. This gives the definitions of SE and SM in formulas (32) and (33) different from formulas (17) and (18).

Reduction of radiation from resonant apertures

To improve the SE due to the presence of an aperture in an infinite metallic screen, we introduce a novel technique that is based on the application of resistive sheets (coating) to the area immediately surrounding the aperture.

The term "loaded aperture" will be used in this work to refer to an aperture coated or surrounded by resistive sheets while maintaining constant aperture size in order to not affect airflow and heat transfer which is a major consideration for enclosures containing high-speed electronics. The resistive sheet concept is depicted in Figure 4.

Incident wave analysis using vector decomposition

In the real case, the plane wave is obliquely incident with the azimuth angle ϕ, elevation angle θ and polarization angle ψ to the θ–axis.[7]

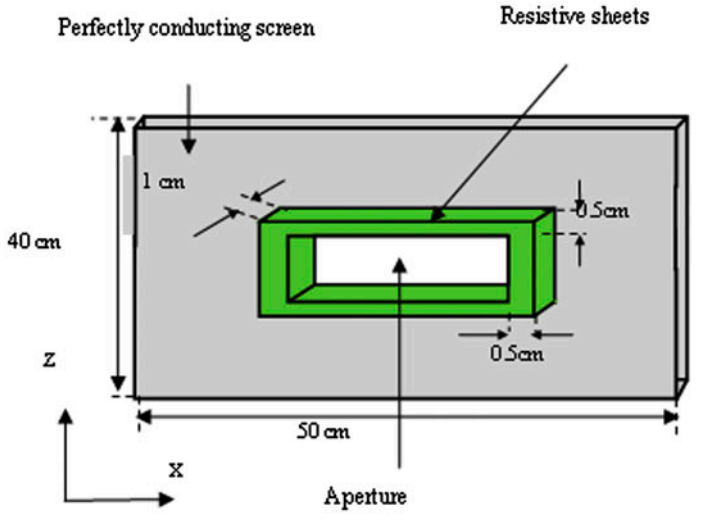

Figure 4. The resistive sheets constituted from an inner frame that is completely contained within the aperture.

Figures 5 and 6 show the obliquely incident wave on the spherical coordinate [15] and the geometry of rectangular enclosure with oblique incident plane wave on aperture.

The electric field E can be decomposed into x, y and z components by simple vector analysis,[16] as follows:

$$\begin{aligned} E = {} & \hat{x}(-\cos\phi\cos\theta\cos\psi - \sin\phi\sin\psi)E_0 + \hat{y}(-\sin\phi\cos\theta\cos\psi + \cos\phi\sin\psi)E_0 \\ & + \hat{z}(\sin\theta\cos\psi)E_0 \\ = {} & \hat{x}Fp_xE_0 + \hat{y}Fp_yE_0 + \hat{z}Fp_zE_0 \end{aligned} \tag{34}$$

where E_0 is the magnitude of E.

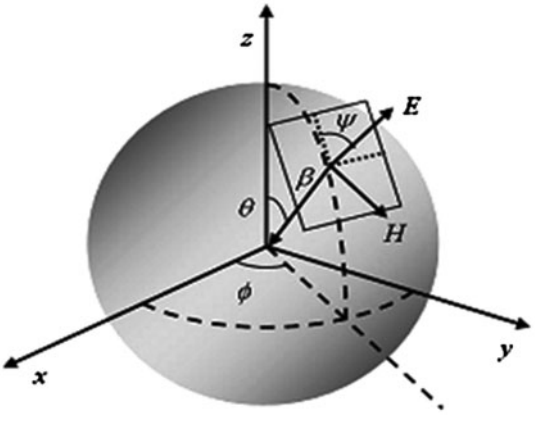

Figure 5. The oblique incident plane wave with the azimuth angle ϕ, elevation angle θ and the polarization angle ψ to the θ axis.

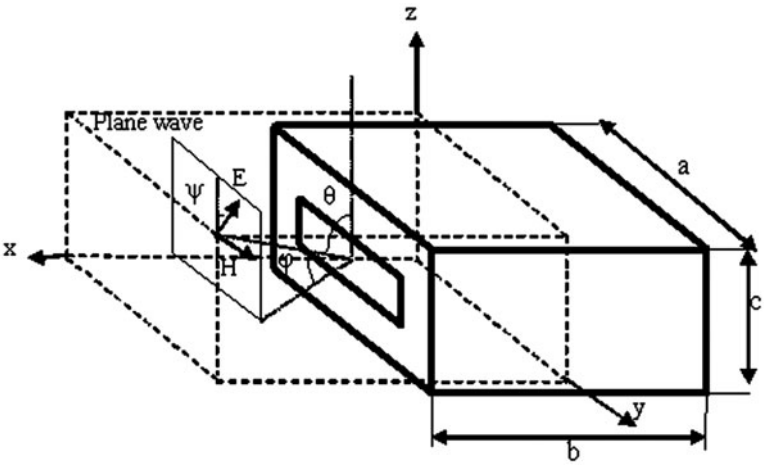

Figure 6. Geometry of the rectangular enclosure with oblique incident plane wave on aperture.

In this equation, the constants of E are defined as factors of polarization Fp_x, Fp_y and Fp_z, which are used for calculating the SE.

The propagation vector β is also given by:

$$\begin{aligned}\beta &= \hat{x}(-\cos\phi\sin\theta)\beta_0 + \hat{y}(-\sin\phi\sin\theta)\beta_0 + \hat{z}(-\cos\theta)\beta_0 \\ &= \hat{x}Fi_x\beta_0 + \hat{y}Fi_y\beta_0 + \hat{z}Fi_z\beta_0\end{aligned} \tag{35}$$

where β_0 is the magnitude of the propagation vector. The constants of β are defined as factors of incidence Fi_x, Fi_y and Fi_z for each direction, which are also used for calculating the SE.

The new relation of SE became:

$$SE_{\text{new}} = Fp_zFi_xSE_{\text{old}} \tag{36}$$

Results and interpretations

Evaluation of the electric and magnetic fields in 3D

The FDTD domain of calculation is clarified in Figure 7. Figures 8 and 9 cover the total area of this metallic enclosure illuminated by a plane wave in the 3D domain.

To assess the effectiveness of the PML (Perfect Math Layer) region, a series of snapshots of the simulation space for Gaussian pulse excitation are plotted. The obtained results summarized in Figures 8 and 9 demonstrate that the PML is adequately effective for absorbing the narrowband. Similar results are reported in [17].

A significant absorption of the electromagnetic wave has been remarked (Figures 8 and 9) at the PML zone. But, at the level of the enclosure, a part of the ELM wave is transmitted while the other one is reflected.

In electromagnetic analysis, various parameters which describe different characteristics are defined in the frequency domain. Therefore, a transformation must be used to convert the fields computed by time-domain methods (like FDTD) into the frequency domain. This transformation is usually performed using a Fourier process such as FFT.[18]

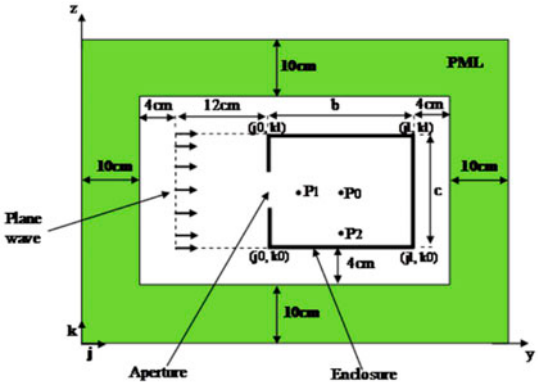

Figure 7. Localization of the enclosure with different positions of calculation.

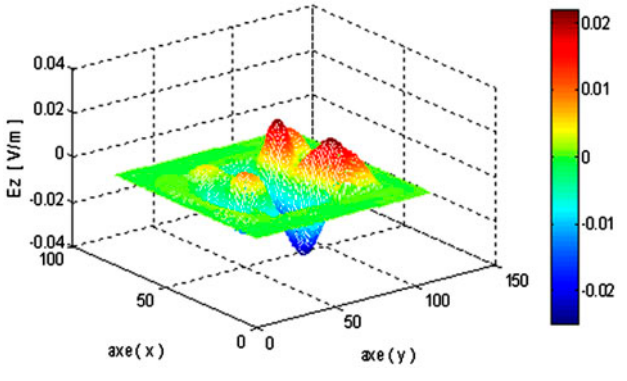

Figure 8. Electric field *Ez* in 3D.

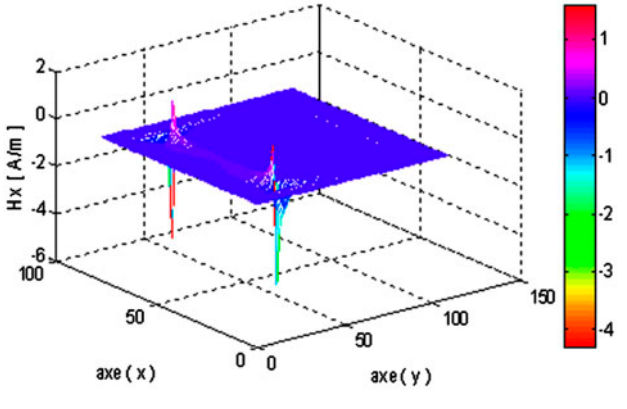

Figure 9. Magnetic field *Hx* in 3D.

SE is computed at the centre of the cavity for a normally incident plane wave. The field at the centre of the enclosure was recorded and submitted to Fourier Transform (Electric field *Ez* with the enclosure). After that, the simulation has been executed for 15,000 time steps, as depicted in Figure 10. For comparison necessity, the electric field *Ez* without enclosure has been also computed. The results are presented in Figure 11.

Electric SE

Firstly, Figure 12 represents the results obtained with and without signal filtering. It illustrates the SE computed by FDTD with Hamming windowing technique.

These picks without filtering are numerical oscillations depending directly on the parameters of simulation (they depend more particularly on the number of iterations as well as on the geometric parameters of the studied structure).

Secondly, the verification of the FDTD numerical method, which compares the SE between our method and CST software/EMC at the middle point P_0 of the box ($25 \times 20 \times 35$ cm), is shown in Figure 1. Very similar results between the three methods are shown. The enclosure resonates at approximately 3.5 MHz, leading to negative shielding (field enhancement) around this frequency (Figure 13). The obtained results can be reinforced by the use of the standard feature selective validation method.[19,20]

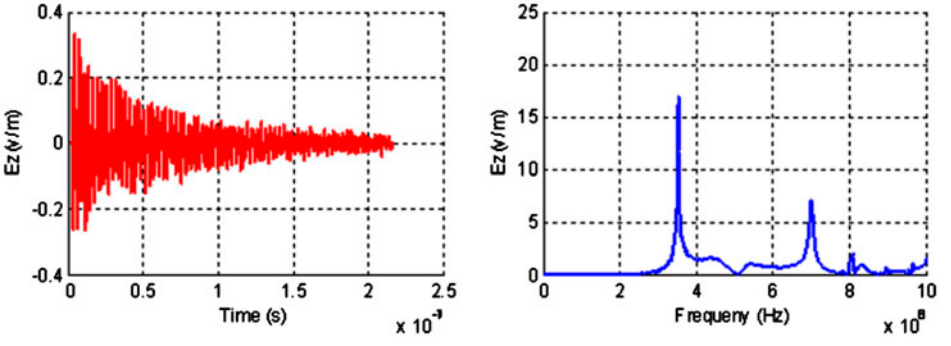

Figure 10. Electric field *Ez* with presence of enclosure.

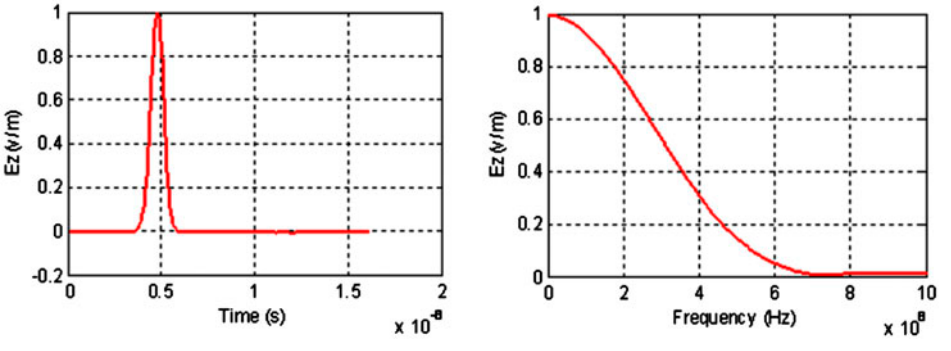

Figure 11. Electric field *Ez* with absence of enclosure.

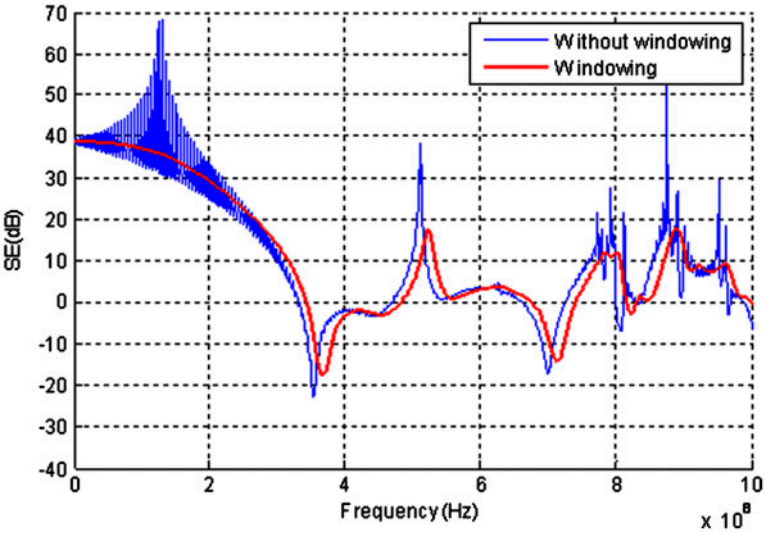

Figure 12. SE with and without Hamming window.

We next proceed to examine the SE for the position of different sampling points (P_0, P_1 and P_2) (Figure 14).[21] In addition, when analysing Figure 15(a), it can be concluded that at lower frequencies, the points which are farther away from the aperture have the better SE. From this conclusion, IC circuit module should be installed as far away as possible from the aperture in the design of electrical systems.

From Figure 15(a), one can observe that for low frequencies, the SE is improved if one moves away the aperture, except at extremely low frequencies. It is mainly owed to the characteristics of the software that has been well adapted to execute simulations at high frequency. This frequency limit depends mainly on the simulated structure and its nature. But in high frequency, we notice the disappearance of certain resonance frequencies at $f = 0.55$ GHz, $f = 0.625$ GHz, $f = 0.635$ GHz, $f = 0.66$ GHz, $f = 0.9$ GHz and $f = 0.98$ GHz.

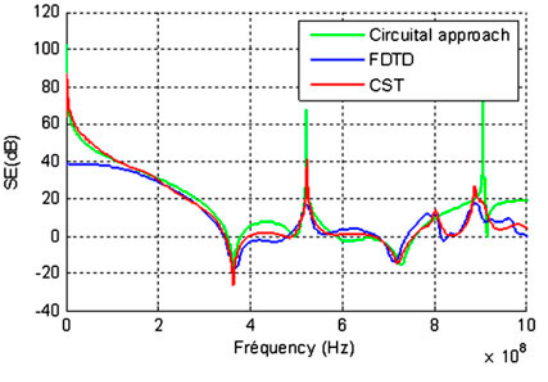

Figure 13. The comparison result of the SE between our method (circuital approach, FDTD) and CST software/EMC.

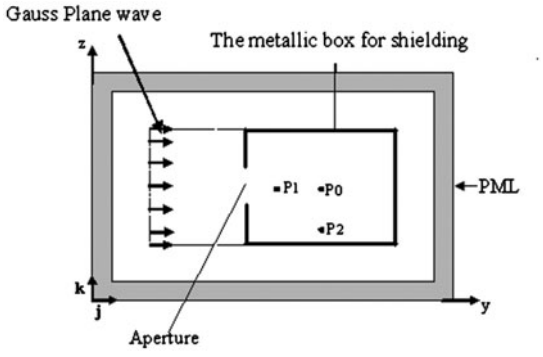

Figure 14. The points at different positions.

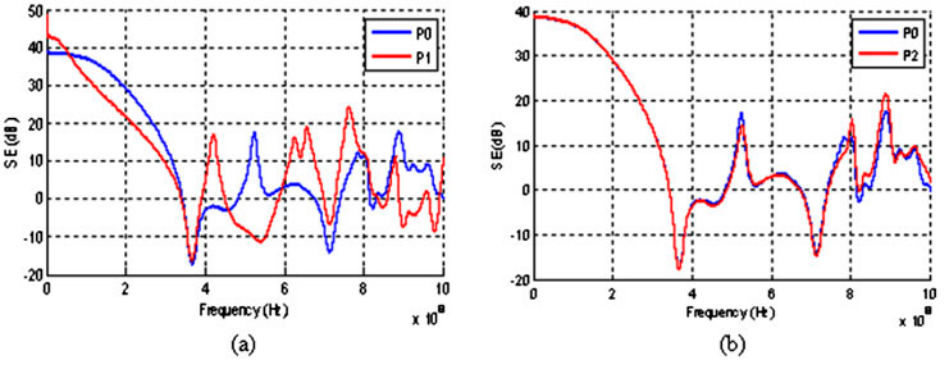

Figure 15. SE of different points, (a) SE of P_0 and P_1, (b) SE of P_0 and P_2.

From Figure 15(b), the SE curves of P_0 and P_2 are almost identical, so the points at equidistance from the wall of the aperture have similar SE.

Magnetic SE

The variations of magnetic shielding effectiveness (SM) have been investigated in the same conditions as SE. Figure 16 depicts the variations of SM for two positions, P_0 (25cm × 20cm × 35 cm) and P (25cm × 20cm × 50 cm) inside the enclosure. It appears that the SM increases with the distance that separates the point of calculation and the aperture (same behaviour than the SE).

Three-dimensions influence on the metal design of the enclosures

The analytical model presents several advantages for SE calculation. Nevertheless, it applies to well definite structures and their application fields are limited. Their utilization depends on the ratio between the characteristic size of the system and the wavelength. Therefore, it does not enable to estimate the behaviour of the electromagnetic shield of different geometries beyond the dimensions proposed in the paper.

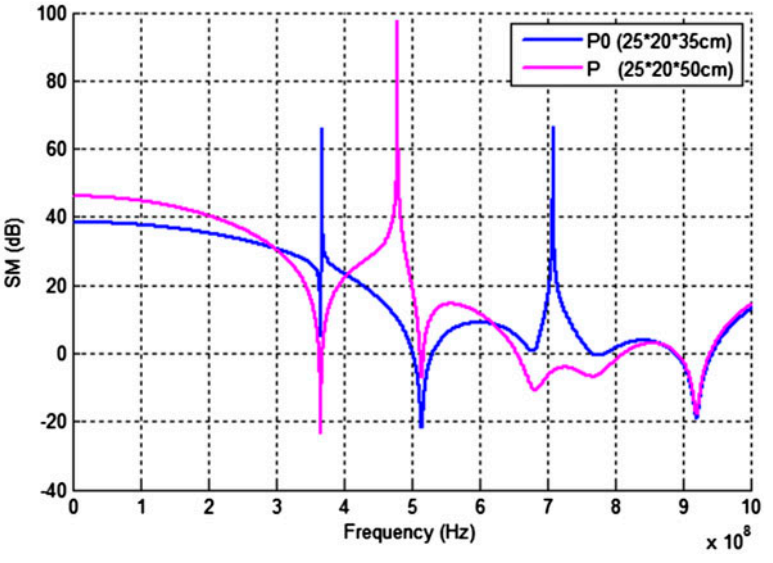

Figure 16. SM in different points (P_0 and P).

For that reason, the commercial CST software and the finite differences method applied to Maxwell's equations have been used as a calculation tools that enable the modelling with an exact formulation of the propagation phenomena and the electromagnetic waves interaction within a given medium.

The goal is to investigate the influence of the changes in the box geometry on the SE. The approach consists of varying separately each of the three dimensions.[22]

Effect of the enclosure length on the SE

To appreciate the effect of the enclosure length on the SE, we preserve the same width and the same height with varying its length. Figure 17 shows the calculated SE and a comparison between two different enclosure lengths with the same aperture. The first one dimension is 50 cm × 40 cm × 70 cm and the second is 50 cm × 40 cm × (70 + 70/2) cm. For larger enclosures, the resonance frequency is lower, with however the appearance of other resonance frequencies.

Effect of the enclosure width on the SE

For the best appreciation of the effect of the enclosure width on the SE, the same length and height have been kept constant while varying the width. Figure 18 shows the calculated SE and the comparison between two different enclosure widths with the same aperture. The first one is 50 cm × 40 cm × 70 cm and the second is (50 + 50/2) cm × 40 cm × 70 cm.

Effect of the enclosure height on the SE

In this part, in order to appreciate the effect of the enclosure height on the SE, we preserve the same length and the same enclosure width while varying its height.

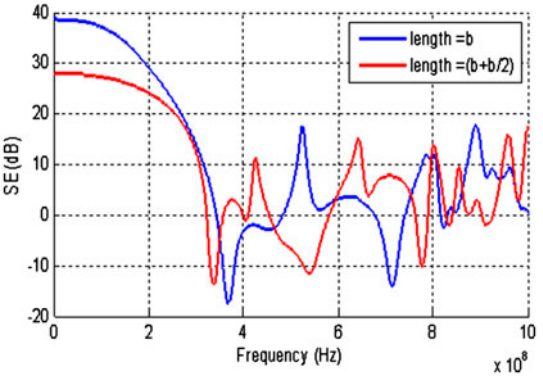

Figure 17. SE with varying the length of the enclosure.

Figure 19 shows the calculated SE with a comparison between two different enclosure heights for the same aperture. The first one is 50 cm × 40 cm × 70 cm and the other is 50 cm × (40 + 40/2) cm × 70 cm.

SE for different aperture shapes

We next proceed to examine the SE of the cavity with a 15.81 cm × 15.81 cm square aperture and a circular (8.92 cm radius) aperture with the same area as a 25 cm× 10 cm rectangular aperture (Figure 20). Through the analysis of the results presented in Figure 21, one may conclude that it is recommendable to use square and circular apertures instead of the rectangular ones when apertures have to be used in shielding boxes. Square or circular apertures can be chosen freely according to practical situation because of the similar SE.[23]

SE for different aperture area

The results obtained from different aperture areas are presented in Figure 22, where it appears that more the aperture is larger, the resonance becomes broader and the low-frequency shielding worsens with regard to smaller apertures.

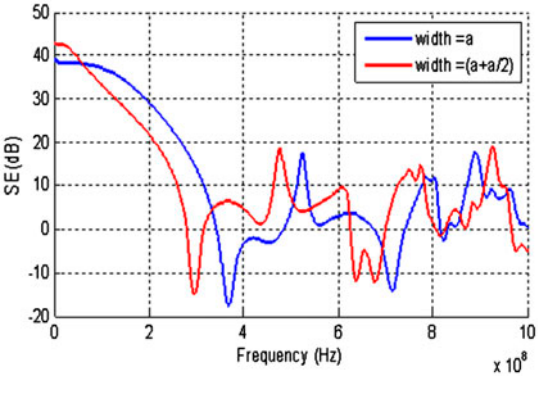

Figure 18. SE with varying the width of the enclosure.

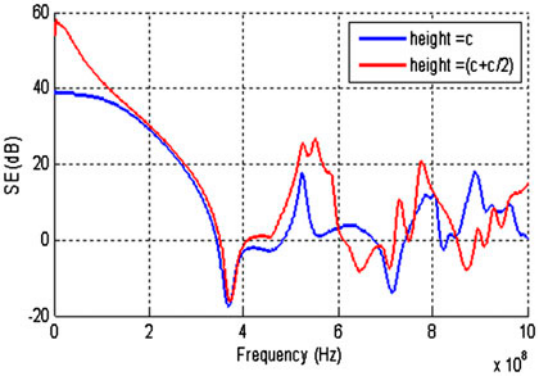

Figure 19. SE with varying the height of the enclosure.

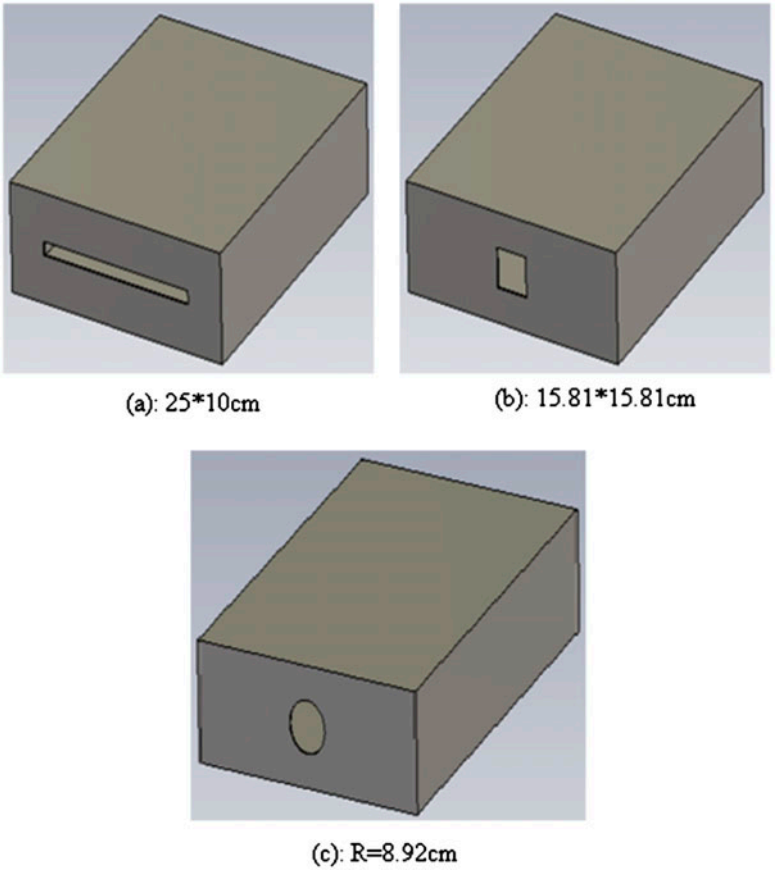

Figure 20. Three geometries for validation, (a) enclosure with a rectangular aperture, (b) enclosure with a square aperture and (c) enclosure with a circular aperture.

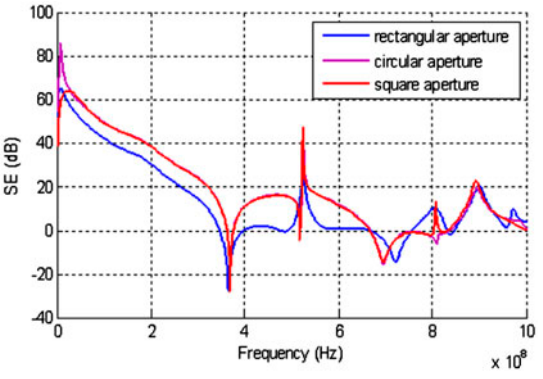

Figure 21. SE of the apertures with different shapes.

SE for rectangular-loaded aperture

The term "loaded aperture" will be used in this work to refer to an aperture coated or surrounded by resistive sheets. The resistive sheet concept is depicted in Figure 4. The use of a resistive sheet constitutes an inner frame of the aperture; it decreases the coupling phenomena created by the induced currents around the aperture. Consequently, it improves the SE and reduces the resonance peaks (Figure 23).

Figure 23 shows the comparison between the resulting SE for the two cases (aperture with and without resistive sheet). We note that there is a significant increase of the SE (especially at high frequency) when the aperture is equipped with a resistive sheet, because this latter made decrease the coupling phenomena appearance through the creation of induced currents around the aperture.

SE for oblique and normal incident plane wave

We have calculated the SE of metallic enclosures with aperture when submitted to an oblique incident arbitrary polarized plane wave. Figure 24 shows that the SE is highly

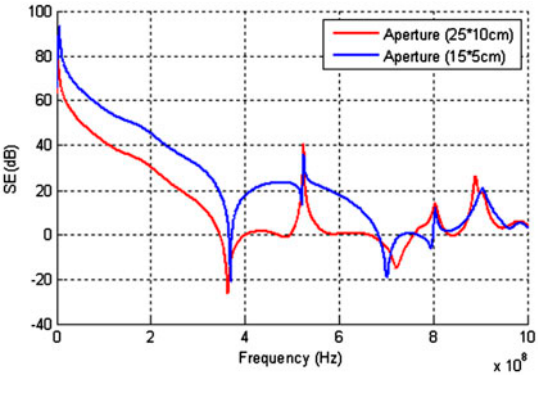

Figure 22. Calculated SE at centre in two 50 cm × 40 cm × 70 cm enclosures with 25 cm × 10 cm and 15 cm × 5 cm aperture.

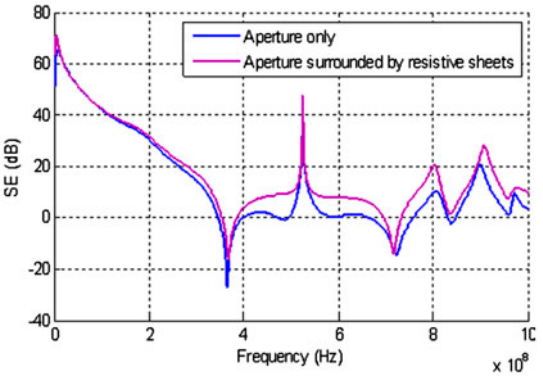

Figure 23. SE of rectangular enclosure with a loaded aperture by resistive sheets.

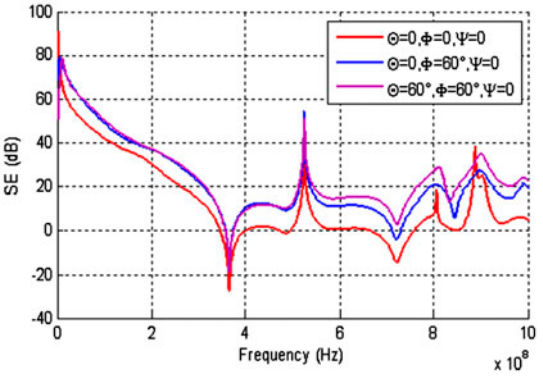

Figure 24. SE as a function of frequency for various θ and φ.

affected by the incidence mode of the plane wave on the metal enclosure with centred aperture that is predictable because it depends on θ and ψ angles.

Conclusion

The SE of a rectangular enclosure has been investigated using the circuital approach, FDTD method and software CST/EMC. Good agreements are found between the results obtained from these techniques. The calculation of electric and magnetic shielding depends on the frequency and polarization of the applied field, the aperture(s) shape, the rectangular-loaded aperture and the position within the enclosure.

Square and circular apertures are preferable to rectangular ones when apertures have to be used in shielding boxes. Square or circular apertures can be chosen freely according to practical situation because of the similar SE. A loss factor has been then successfully introduced to describe the resonances in direct relation with the enclosure. The formulation can be useful to designers of shielded enclosures.

References

[1] Robinson MP, Benson TM, Christopoulos C, Dawson JF, Ganley MD, Marvin AC, Porter SJ, Thomas DWP. Analytic formulation for the shielding effectiveness of enclosure with apertures. IEEE Trans. EMC. 1998;40:240–248.

[2] Argus P, Fischer P, Konrad A, Schwab AJ. Efficient modeling of apertures in thin conducting screens by the TLM method. Paper presented at: IEEE International Symposium on Electromagnetic Compatibility; 2000 Aug 21–25; Washington, DC.

[3] Taflove A, Umashankar KR, Beker B, Harfoush F, Yee KS. Detailed FD-TD analysis of electromagnetic fields penetrating narrow slots and lapped joints in thick conducting screens. IEEE Trans. Antennas Propag. 1988;36:247–257.

[4] Li M, Nuebel J, Drewniak JL, Hubing TH, DuBroff RE, Van Doren TP. EMI from cavity modes of shielding enclosures – FDTD modeling and measurements. IEEE Trans. Electromagn. Compat. 2000;42:29–38.

[5] Wang MY, Xu J, Wu J, Yan Y, Li HL. FDTD study on scattering of metallic column covered by double negative metamaterial. J. Electromagn. Waves Appl. 2007;21:1905–1914.

[6] Clemens M, Feigh S, Weiland T. Geometric multigrid algorithms using the conformal finite integration technique. IEEE Trans. Magn. 2004;40:1065–1068.

[7] Shim J, Kam DG, Kwon JH, Kim J. Circuital modeling and measurement of shielding effectiveness against oblique incident plane wave on apertures in multiple sides of rectangular enclosure. IEEE Trans. EMC. 2010;52:566–577.

[8] Benhassine S, Pichon L, Tabbara W. An efficient finite-element time-domain method for the analysis of the coupling between wave and shielded enclosure. IEEE Trans. Magn. 2002;38:709–712.

[9] Taflove A, Umashankar K. A hybrid moment method/finite-difference time-domain approach to electromagnetic coupling and aperture penetration into complex geometries. IEEE Trans. Antennas Propag. 1982;30:617–627.

[10] Feng C, Shen Z. A hybrid FD–MoM technique for predicting shielding effectiveness of metallic enclosures with apertures. IEEE Trans. Electromagn. Compat. 2005;47:456–462.

[11] Gupta KC, Garg R, Bahl IJ. Microstrip lines and slotlines. Norwood, MA: Artech House; 1979.

[12] Ma KP, Li M, Drewniak JL, Hubing TH, Van Doren TP. Comparison of FDTD algorithms for subcellular modeling of slots in shielding enclosures. IEEE Trans. Electromagn. Compat. 1997;39:147–155.

[13] Chaoqun Jiao, Lin Li, Xiang Cui, Huiqi Li. Subcell FDTD analysis of shielding effectiveness of a thin-walled enclosure with an aperture. IEEE Trans. Magn. 2006;42:1075–1078.

[14] Georgakopoulos SV, Birtcher CR, Balanis CA. HIRF penetration through apertures: FDTD versus measurements. IEEE Trans. EMC. 2001;43:282–294.

[15] Shi D, Shen Y, Ruan F, Wei Z, Gao Y. Shielding analysis of enclosure with aperture irradiated by plane wave with arbitrary incident angle and polarization direction. Paper presented at: IEEE EMC 2008. International Symposium on Electromagnetic Compatibility; 2008 Aug 18–22; Detroit, MI.

[16] Shim J, Kam DG, Kwon JH, Choi HD, Kim J. Circuital approach to evaluate shielding effectiveness of rectangular enclosures with apertures on multiple sides. Paper presented at: IEEE EMC Europe 2004. International Symposium on Electro-Magnetic Compatibility; 2004 Sep 7; Eindhoven, The Netherlands.

[17] Berenger JP. A perfectly matched layer for the absorption of electromagnetic waves. J. Comput. Phys. 1994;114:185–200.

[18] Park JK, Shin DH, Lee JN, Eom HJ. A fullwave analysis of a coaxial waveguide slot bridge using the Fourier transform technique. J. Electromagn. Waves Appl. 2006;20:143–158.

[19] Duffy AP, Martin AJM, Orlandi A, Antonini G, Benson TM, Woolfson MS. Feature selective validation (FSV) for validation of computational electromagnetics (CEM). Part I – The FSV method. IEEE Trans. Electromagn. Compat. 2006;48:449–459.

[20] Orlandi A, Duffy AP, Archambeault B, Antonini G, Coleby DE, Connor S. Feature selective validation (FSV) for validation of computational electromagnetics (CEM). Part II – assessment of FSV performance. IEEE Trans. Electromagn. Compat. 2006;48:460–467.

[21] Olyslager F, Laermans E, De Zutter D, Criel S, De Smedt R, Lietaert N, De Clercq A. Numerical and experimental study of the shielding effectiveness of a Metallic enclosure. IEEE Trans. Electromagn. Compat. 1999;41:202–213.

[22] Azizi H, Tahar Belkacem F, Moussaoui D, Bensetti M. Numerical study for the shielding effectiveness of a rectangular enclosure with apertures. Paper presented at: EMC Europe 2012. International Symposium on Electromagnetic Compatibility; 2012 Sep 17–21; Roma, Italy.
[23] Tahar Belkacem F, Boutar A, Bensetti M, Duval F, Djennah M, Mazari B. The analytical and numerical evaluation versus experimental of electromagnetic shielding effectiveness of a rectangular enclosure with apertures. Paper presented at: 19th Soft Magnetic Materials Conference; 2009 Sep 6–9; Torino, Italy.